Published online 25 September 2007 *Nucleic Acids Research, 2007, Vol. 35, No. 19* **6501–6516**
doi:10.1093/nar/gkm608

Generation of a transgenic zebrafish model of Tauopathy using a novel promoter element derived from the zebrafish *eno2* gene

Qing Bai[1,2], Jessica A. Garver[1,2], Neil A. Hukriede[3] and Edward A. Burton[1–5,*]

[1]Pittsburgh Institute for Neurodegenerative Diseases, [2]Department of Neurology, [3]Department of Molecular Genetics and Biochemistry, University of Pittsburgh School of Medicine, [4]Department of Neurology, Pittsburgh VA Healthcare System and [5]Division of Movement Disorders, University of Pittsburgh Medical Center, Pittsburgh, PA, USA

Received May 8, 2007; Revised July 25, 2007; Accepted July 26, 2007

ABSTRACT

The aim of this study was to isolate *cis*-acting regulatory elements for the generation of transgenic zebrafish models of neurodegeneration. Zebrafish enolase-2 (*eno2*) showed neuronal expression increasing from 24 to 72 h post-fertilization (hpf) and persisting through adulthood. A 12 kb *eno2* genomic fragment, extending from 8 kb upstream of exon 1 to exon 2, encompassing intron 1, was sufficient to drive neuronal reporter gene expression *in vivo* over a similar time course. Five independent lines of stable Tg(*eno2:GFP*) zebrafish expressed GFP widely in neurons, including populations with relevance to neurodegeneration, such as cholinergic neurons, dopaminergic neurons and cerebellar Purkinje cells. We replaced the *exon 2-GFP* fusion gene with a cDNA encoding the 4-repeat isoform of the human microtubule-associated protein Tau. The first intron of *eno2* was spliced with high fidelity and efficiency from the chimeric *eno2-Tau* transcript. Tau was expressed at ~8-fold higher levels in Tg(*eno2:Tau*) zebrafish brain than normal human brain, and localized to axons, neuropil and ectopic neuronal somatic accumulations resembling neurofibrillary tangles. The 12 kb *eno2* promoter drives high-level transgene expression in differentiated neurons throughout the CNS of stable transgenic zebrafish. This regulatory element will be useful for the construction of transgenic zebrafish models of neurodegeneration.

INTRODUCTION

The zebrafish has shown great utility as a model organism for studying the molecular mechanisms of vertebrate development. The rapid external development and transparency of zebrafish embryos allow direct observation of developmental processes and the deployment of fluorescent reporter genes to facilitate examination of spatial and temporal gene expression patterns in living embryos (1,2). The availability of efficient techniques for manipulation of gene expression enables studies of gene function to be executed readily (3). The ease with which genetic and small molecule screens can be carried out has allowed the identification of novel genetic pathways involved in specific developmental processes and the isolation of novel chemical modifiers (4–7). More recently, it has been suggested that many of these advantages might apply to the study of human diseases: valuable insights into disease pathogenesis, or leads to new therapeutic approaches, could be provided by high-content small molecule screens, genetic suppressor screens, observation of disease progression in real time *in vivo*, using fluorescent reporters to label cell populations of interest, and rapid hypothesis-testing experiments in statistically robust samples of larvae (8–10). Exploitation of these techniques could provide powerful means to analyse human disease. However, full realization of this potential will be critically dependent on the development of zebrafish models that faithfully recapitulate relevant pathological mechanisms.The long-term objectives of our work are to elucidate mechanisms of neurodegeneration and to identify novel neuroprotective compounds to treat patients with neurodegenerative diseases. We aim to accomplish these objectives by exploiting the advantageous features of the zebrafish as a model. The zebrafish is an appropriate organism in which to study neurodegeneration. As a vertebrate, the basic organization and divisions of the nervous system are similar to those of other vertebrates, including humans (11). The zebrafish CNS contains specialized neuronal populations of direct relevance to human neurodegenerative diseases, for example, dopaminergic neurons (12), cerebellar Purkinje cells (13) and

*To whom correspondence should be addressed. Tel: +1 4126488480; Fax: +1 4126489082; Email: eab25@pitt.edu

motor neurons (14). In addition to neurons, the zebrafish CNS contains oligodendrocytes (15) and astrocytes (16), the human homologues of which may play central roles in neurodegeneration through critical neural–glial interactions. Finally, there is extensive genetic and biochemical similarity between the zebrafish and human. Many genes involved in human neurodegenerative diseases have highly conserved orthologues in the zebrafish (17–19). Zebrafish neurons are susceptible to toxins that target pathways implicated in sporadic neurodegenerative diseases (20–23). These considerations suggest that it may be possible to recapitulate neurodegeneration in the zebrafish brain through similar biochemical mechanisms to those underlying human disease. Consequently, generation of representative disease models may be feasible, enabling the analyses described above to yield insights into pathogenic mechanisms and identification of therapeutic targets.

As a first step towards developing zebrafish models of neurodegenerative disease, we would like to test the hypothesis that zebrafish, engineered to express genes associated with neurodegeneration in humans, will develop histological and biochemical abnormalities reflecting those found in the relevant diseases. This hypothesis can be tested by generating transgenic zebrafish expressing appropriate genes in CNS neurons, and then carrying out analysis for evidence of neuronal cell death or dysfunction, and histopathological features or biochemical abnormalities reminiscent of the human diseases. Generation of transgenic models relies on the availability of *cis*-acting regulatory elements that drive transgene expression in an appropriate spatial and temporal pattern. For a neurodegenerative disease model, the regulatory elements should have the following properties: (i) expression in a wide variety of neurons, in order to study the differential vulnerability of specific neuronal subpopulations, which is a key feature of human diseases; (ii) expression commencing in differentiated neurons after the earliest stages of development, since a pathogenic transgene might provoke pathological changes in neuronal precursors through disruption of developmental mechanisms that are not relevant to late-onset neurodegeneration; (iii) expression persisting into adulthood, in order to examine the effects of aging on pathogenesis and disease progression; (iv) expression that is sufficiently robust to provoke a phenotype. The purpose of the present study was to isolate suitable *cis*-acting regulatory elements with these properties.

Mammals have three forms of the glycolytic enzyme enolase, each encoded by a separate gene. The mammalian ENO2 gene encodes the neuron-specific γ-enolase isoenzyme (24), which is expressed in mature neurons throughout the neuraxis; consequently, neuron-specific enolase (NSE) is frequently used as a marker to identify cells with neuronal differentiation in human histopathology samples (24). A 1.8 kb fragment of the rat ENO2 promoter drives transgene expression widely in mature neurons of the mouse CNS (25) and has been used to generate transgenic rodent models for the study of neurodegeneration (26–31). Since endogenous zebrafish promoters have been associated with high transgenesis rates and reproducible expression patterns (32), we decided to clone the zebrafish orthologue of ENO2 and to isolate its promoter as a resource for generating transgenic models of neurodegeneration in zebrafish.

In this study, we identified and characterized the zebrafish *eno2* gene. Zebrafish *eno2* is first expressed in the developing nervous system at 24 hpf; however, steady-state levels of the transcript become significantly more abundant later during development and robust expression persists through adulthood. We isolated the zebrafish *eno2* promoter region, and showed that its activity in driving GFP reporter gene expression *in vivo* was enhanced by the presence of the first intron, which contains a putative CpG island. Five independent lines of Tg(*eno2:GFP*) zebrafish, in which green fluorescent protein was expressed under the transcriptional control of a 12 kb zebrafish *eno2* promoter fragment, showed widespread neuronal GFP expression, including cholinergic, dopaminergic GABAergic and cerebellar Purkinje neurons. In order to assess the utility of this promoter element for constructing disease models, we replaced GFP with a cDNA expressing the 4-repeat isoform of the human microtubule-associated protein Tau. Stable transgenic Tg(*eno2:Tau*) zebrafish showed widespread CNS neuronal expression of Tau, at high levels compared with normal human brain. Human 4R-Tau was found within axons, neuropil and in ectopic accumulations in neuronal cell bodies of Tg(*eno2:Tau*) zebrafish. These data show that *cis*-acting elements from the zebrafish *eno2* regulatory region will be useful for stable expression of transgenes in neurons throughout the zebrafish CNS. The *eno2* promoter will enable us to test the hypothesis that biochemical and histological changes representative of human diseases may be provoked in susceptible neuronal populations by expression of mutant transgenes.

MATERIALS AND METHODS

Zebrafish and microscopy

Experiments were carried out in accordance with Institutional Animal Use and Care Committee regulations and approvals. Adult stocks of strain AB* zebrafish were maintained at 28.5°C and euthanized by deep tricaine anaesthesia followed by exposure to ice-cold water. Embryos were raised in E3 buffer (5 mM NaCl, 0.17 mM KCl, 0.33 mM $CaCl_2$, 0.33 mM $MgSO_4$). Microscopy was carried out after tricaine anaesthesia to prevent movement. Images of free-floating whole larvae were obtained using an inverted microscope, and confocal images were obtained after embedding anaesthetized larvae in 3% low melting point agarose in E3 buffer.

Northern blot

RNA was separated on a 1.2% agarose formaldehyde/MOPS gel and transferred to Nytran-N membrane (Schleicher & Schuell BioScience, Keene, NH). *eno2* antisense cRNA probe was generated by *in vitro* transcription of a plasmid template containing 307 bp of the *eno2* open reading frame and 5′UTR using digoxigenin-conjugated UTP to label the antisense cRNA probe (Roche, Indianapolis, IN, USA).

Pre-hybridization was carried out in UltraHyb (Ambion, Austin, TX< USA) supplemented with Torula RNA (1 mg/ml final concentration; Sigma, St Louis, MO, USA), followed by addition of cRNA probe (20 ng/ml final concentration) to the hybridization buffer. Blots were washed in 2× SSC, 0.1% SDS and 0.1× SSC, 0.1%, SDS. Probe was detected with alkaline-phosphatase (AP) conjugated anti-DIG FAb (Roche, Indianapolis, IN, USA), in maleic acid buffer, 1% blocking substrate, and revealed by exposure to photographic film after incubation with a light-emitting AP substrate (*CDP-star*, Roche, Indianapolis, IN, USA).

Whole mount mRNA *in situ* hybridization

Embryos were raised in E3 buffer, 0.003% 1-phenyl-2-thiourea to prevent pigment formation, fixed overnight at 4°C in 4% paraformaldehyde (PFA) in phosphate-buffered saline pH 7.5 (PBS), washed in PBS, dehydrated in methanol and stored at –20°C. Prior to hybridization, embryos were treated with acetone at –20°C, re-hydrated in 50 and 30% methanol and then diethylpyrocarbonate (DEPC)-treated PBS, followed by protease-K (10 µg/ml) at room temperature for 5–30 min, followed by post-fixing in 4% PFA and washing in PBTw (PBS, 0.1% Tween-20, 0.2% bovine serum albumin). Pre-hybridization was carried in 50% formamide, 2× SSC, 0.3% 3-[(3-cholamidopropyl)dimethylammonio]-1-propanesulphonate (CHAPS), 1 mg/ml torula RNA, 50 µg/ml heparin, followed by the addition of 150 ng/ml cRNA probe. Embryos were washed in 50% formamide, 2× SSC, 0.3% CHAPS, then 2× SSC, 0.3% CHAPS, followed by 0.2× SSC, 0.3% CHAPS. Probe was detected using AP conjugated anti-DIG antibody diluted in maleic acid buffer, and revealed by incubation in BM Purple (Roche, Indianapolis, IN).

mRNA *in situ* hybridization in brain sections

Zebrafish brains were fixed in 4% PFA at 4°C for 6 h, washed with PBS and cryoprotected in PBS-sucrose. Ten micrometer thick cryosections on SuperFrost slides (Fisher, Pittsburgh, PA), were post-fixed in 4% PFA, carbethoxylated with 0.1% DEPC in PBS (33), washed in 5× SSC, and post-fixed in 4% PFA. Following incubation in hybridization buffer (UltraHyb, Ambion, Austin, TX) supplemented with Torula RNA (4 mg/ml final concentration; Sigma, St Louis, MO) for 1 h at 68°C, DIG-labelled RNA probe (final concentration 0.2 ng/µl) was added to the buffer and sections were incubated in a humid chamber overnight at 68°C, following which they were washed in 2× SSC, 1× SSC then 0.1× SSC. Probe was detected using an AP-conjugated anti-DIG FAb diluted 1:1000 in maleic acid buffer, 1% blocking substrate (Roche), and revealed by incubation in a colorigenic AP substrate (*BM-Purple*, Roche, Indianapolis, IN, USA).

RT–PCR, 5′RACE and 3′RACE

For RT–PCR, total RNA from whole adult zebrafish brains was subjected to reverse transcription using *SuperScript III* (Invitrogen, Carlsbad, CA, USA). PCR amplification was carried out using primers complementary to *eno2* exon1 F: 5′-CGC TCT GTT TTC CTC TCT CTT CCG-3′ and Tau R: 5′-AAT CCT GGT GGC GTT GGC CT-3′; beta actin F: 5′- ATG GAT GAG GAA ATC GCT GC-3′ and R: 5′- AGC CTC AGT GAG CAC GAC AG-3′; *eno2* F: 5′-ATG TCT GTT GTA AGC ATC AT -3′ and R: 5′-GAT GTG TCT GTC TGC ATT TG -3′. 5′ and 3′ RACE were carried out as described (17), using zebrafish *eno2* primers 3′RACE: 5′-ATC TGA GCG TCT CGC CAA AT-3′, and 5′RACE: 5′-ATG ATG GCT GGC CCG AGA GTG T-3′. Products were cloned in pGEM-T (Promega, Madison, WI, USA) and sequenced. Multiple sequences were aligned and compared using *AlignX*.

DNA constructs

An EcoRI/AflII restriction fragment containing eGFP-poly(A) was obtained by digestion of pEGFP-1 (Clontech, Mountain View, CA, USA), and ligated into the EcoRI/PmeI sites of pBluescript SK-I-Sce1 (a kind gift from Dr Michael Tsang, University of Pittsburgh) to make pBS-I-Sce1-GFP. Homologous zebrafish *eno2* arms were amplified from BAC zC51M24 (CHORI21 library) by PCR using primers 5′-GGA ATT CCA TCA CAA TGT ATC AGC-3′ and 5′-GTA CCC ATG GCA ATG ATG CTT ACA AC-3′ (3′arm; *eno2* exon 2) and 5′-GGG GTA CCT GTT AGT AAA GGC AGA T-3′ and 5′-A ATT CAA TGG CAC GTT TGA TCG-3′ (5′arm; *eno2* 5′ genomic flanking sequence). The homologous arms were inserted into the EcoRI/NcoI sites (3′ arm) or KpnI/EcoRI sites (5′ arm) of pBS-I-Sce1-GFP, such that the eGFP ORF was in frame with exon 2 from the zebrafish *eno2* gene. The resulting plasmid was verified by restriction digest and direct DNA sequencing, and then linearized by EcoRI digest. A 12 kb fragment of the *eno2* gene was captured from BAC zC51M24 using gap repair recombination (the inducible bacterial strains for carrying out the recombination were a kind gift from Dr Neal Copeland, NCI). DY380 cells were transformed with BAC zC51M24 by electroporation. DY380-BACzC51M24 cells were grown at 32°C to $OD_{590} = 0.5$ then induced at 42°C for 15 min before being transformed with linearized plasmid by electroporation. Recombinants were identified by ampicillin resistance, and verified by restriction digest and direct DNA sequencing. A similar strategy was used for cloning the *eno2:4R-Tau* gene cassette, except that the Tau ATG replaced the zebrafish *eno2* ATG in order to preserve the N-terminus of the resulting protein. The homologous arms were generated by PCR amplification from BAC zC51M24, using the following primers: 5′-GGG GTA CCT GTT AGT AAA GGC AGA TTC-3′ and 5′-CCG CTC GAG TCC ACA TTA CCT TCT GTT G-3′ (5′ arm; *eno2* 5′genomic flanking sequence), and 5′-CCG CTC GAG TCC ATC ACA ATG TAT CAG C-3′ and 5′-CTC ACC ATG GCA ATG ATG CTT ACA ACA GAA GGC CTT AAA GAC AAG-3′ (*eno2* intron 1), and cloned into the XhoI/NcoI sites (5′ arm) or KpnI/XhoI sites of pBS-I-Sce1-GFP. The open reading frame of human 4-repeat Tau was amplified from plasmid t2 (a kind gift from Dr Matthew Farrer, Mayo Clinic,

Jacksonville, Florida) by PCR using primers 5′-ATG GCT GAA CCC CGA CAG GAG-3′ and 5′-GAC CCA TGG ATC CTC ACA AAC CCT GCT TGG C-3′, and cloned into the StuI/NcoI sites of pBS-I-Sce1-eno2-GFP. The IRES sequence derived from pIRES2-eGFP (Clontech) was inserted into the BamHI/NcoI sites of pBS-I-Sce1-eno2:Tau-GFP. The resulting plasmid was linearized using XhoI prior to transformation and recombination, as described above.

Transgenic zebrafish

A restriction digest containing the following components was prepared on ice: plasmid DNA (pBS-I-Sce1-eno2:GFP, or pBS-I-Sce1-eno2:Tau-IRES-GFP) 0.6 μg, injection dye (0.5% phenol red, 240 mM KCl, 40 mM HEPES pH 7.4) 1 μl, 10× I-Sce1 buffer (100 mM Tris–HCl, 100 mM MgCl2, 10 mM Dithiothreitol, pH 8.8) 0.5 μl, I-Sce1 (New England Biolabs) 1 μl (5 U), ddH_2O to total 10 μl. Single cell embryos were microinjected with 0.5 nl of the restriction digest reaction, containing 30 pg DNA, using a glass micropipette. All surviving fish were raised to sexual maturity and crossed in pairs to identify germline chimeras. The genotype of progeny embryos of F0 pBS-I-Sce1-eno2:GFP and pBS-I-Sce1-eno2:Tau-IRES-GFP microinjected fish was determined by PCR of pooled embryo lysate genomic DNA using primers 5′-CGT AAA CGG CCA CAA GTT CAG C-3′ and 5′-CGA TGT TGT GGC GGA TCT TGA AG-3′. Pairs of fish that transmitted the transgene to progeny embryos were then outcrossed to wild-type fish and embryo genotyping repeated, in order to determine which one of each pair was the germline chimera. F1 progeny of each germline F0 fish were then raised to adulthood. Tg(*eno2:GFP*) F1 fish were identified by epifluorescence microscopy of F2 embryos after outcross to wild-type fish. Tg(*eno2:4R-Tau*) fish were identified by PCR of genomic DNA extracted from tail fin. Two- to three-month-old fish were anaesthetized in 4% tricaine (Acros). A small segment of caudal fin was excised and incubated in 100 μl of DNA extraction buffer [10 mM Tris pH 8.0, 10 mM EDTA, 200 mM NaCl, 0.5% SDS and 200 ug/ml proteinase K (Invitrogen)] at 55°C for 3 h. The sample was then heated to 100°C for 5 min to inactivate proteinase K, and 0.6 μl of each sample was used as a template for PCR using the GFP primers shown above. Each line of transgenic fish was derived from a single F1 founder, and each F1 founder was derived from a single F0 germline chimera. Stocks were maintained by genotyping as above. The data reported here are derived from F2, F3 and F4 generation zebrafish.

Immunohistochemistry (IHC) and immunofluorescence

Adult fish brains were dissected and fixed in 4% PFA, followed by cryoprotection in PBS-sucrose. Cryosections measuring 20 μm were incubated overnight at 4°C with primary antibody, diluted: 1:500 (GFP; cat# MAB3580 Chemicon, Temecula, CA, USA), 1:250 (ChAT; cat# AB144P, Chemicon; this antibody was incubated with sections for 72 h at 4°C), 1:100 (IP3R1; cat#ACC-019, Alomone Labs, Jerusalem, Israel), 1:1000 (GABA; cat# A2052, Sigma), 1:500 (Human Tau; cat#AHB0042, Biosource, Camarillo, CA, USA) or 1:500 (TH; cat# AB152, Chemicon), in carrier buffer (PBS, 1% goat or donkey serum, 1% BSA). For IHC, a biotinylated anti-mouse secondary antibody (2 μg/ml; cat# BA-2000, Vector Laboratories, Burlingame, CA, USA) was diluted 1:200 in carrier buffer, followed by staining in NovaRed (Vector Laboratories) and counterstaining in Mayer's haematoxylin (Sigma, St Louis, MO, USA). For immunofluorescence, primary antibodies were detected using Alexa-488 (anti mouse) and Alexa-555 (anti-rabbit or goat) conjugated secondary antibodies (Invitrogen, Carlsbad, CA, USA), diluted 1:2000 in carrier buffer.

Western blot

Whole brains from 3-month-old zebrafish were sonicated in RIPA lysis buffer (50 mM Tris, pH 8.0, 150 mM NaCl, 1% NP-40, 5 mM EDTA, 0.5% sodium deoxycholate and 0.1% SDS), in the presence of protease inhibitors (complete mini, Roche, Indianapolis, IN, USA) on ice. The homogenate was centrifuged at 20 000*g* for 20 min at 4°C. The protein concentration of each brain extract was determined by Bradford assay and 10 μg was loaded onto 12% SDS-PAGE after boiling in SDS sample buffer, and electroblotted onto PVDF membrane (Bio-Rad). The membrane was blocked in 150 mM NaCl, 100 mM Tris–HCl pH 7.5, 0.1% Tween-20 (TBST), 10% dried non-fat milk for 60 min at room temperature, probed with mouse monoclonal anti-Tau antibody (1:500, cat#AHB0042, Biosource, Camarillo, CA, USA) or polyclonal anti-actin antibody (1:1000; cat#A2066, Sigma, St Louis, MO, USA) overnight at 4°C in TBST, 10% milk, washed in TBST, and bound antibody detected using an HRP conjugated secondary antibody (goat anti-mouse, cat# 31430, Pierce, Rockford, IL; goat anti-rabbit, cat# 4010-05, Southern Biotech, Birmingham, AL) diluted 1:10,000 in TBST and chemiluminescent substrate (ECL, Amersham Biosciences, Chalfont, UK).

RESULTS

Identification and expression pattern of zebrafish *eno2*

A *TBLASTN* search of the zebrafish genome, using the amino acid sequence of human γ-enolase as a probe, identified four gene loci encoding proteins with homology to γ-enolase, located on zebrafish chromosomes 2, 19, 22 and 23. Further database searches identified ESTs and mRNAs corresponding to each of these four genes, but no additional zebrafish enolase sequences were found. The protein sequences predicted by the four zebrafish genes were aligned with the primary sequences of human, rat and mouse α-, β- and γ-enolases and evolutionary relationships between the proteins were inferred by construction of a dendrogram using the neighbour joining method of Saitou and Nei (34). The enolase encoded by the zebrafish chromosome 19 gene locus was most closely related to human and rodent γ-enolases (Figure 1A). We refer to this zebrafish gene as *eno2* and its product as γ-enolase. Human and zebrafish γ-enolases showed 84% identity and 92% similarity (Figure 1B). The enolase

Figure 1. The zebrafish *eno2* orthologue. (**A**) Four zebrafish enolase genes identified by BLAST search were located on chromosomes 2, 19, 22 and 23. The predicted amino acid sequences encoded by each of these genes were aligned with the human, rat and mouse α-, β- and γ-enolase sequences using the *AlignX* implementation of the *ClustalW* algorithm. The dendrogram shown was generated using the neighbour joining method of Saitou and Nei (34). The inferred evolutionary relationships between the zebrafish genes and their mammalian orthologues suggest that zebrafish γ-enolase is encoded by the chromosome 19 gene locus, to which we refer as '*eno2*' throughout the remainder of the article. (**B**) An alignment of zebrafish γ-enolase with human γ-enolase is shown. Non-similar amino acid substitutions are shaded black and conservative substitutions are shaded grey.

encoded by the zebrafish chromosome 2 locus was most closely related to mammalian β-enolases, suggesting that this gene should be designated zebrafish *eno3*. The enolases encoded by the zebrafish chromosome 22 and chromosome 23 gene loci were highly homologous to one another, and to mammalian α-enolases, suggesting that there are two zebrafish *eno1* genes.

We cloned the zebrafish *eno2* transcript from adult brain by RT–PCR (data not shown), confirming the sequence of the transcript and predicted protein, and enabling generation of cRNA probes for expression pattern studies. Hybridization of an *eno2* antisense cRNA probe with a northern blot containing total RNA from adult zebrafish brain, muscle and gut revealed a single brain-specific *eno2* mRNA of 3.5 kb (Figure 2A). RNA *in situ* hybridization was used to localize expression of the *eno2* transcript within the adult brain (Figure 2B). The *eno2* antisense cRNA probe hybridized with cells that showed neuronal morphology (Figure 2B, inset panel) and were located in grey matter nuclei and laminae throughout the brain and spinal cord (Figure 2B, upper two panels). The most prominent labelling was seen in the telencephalon, deep laminae of the optic tectum, cranial nerve motor nuclei, granule cell and Purkinje cell layers of the cerebellum and brainstem reticular formation. Under identical conditions, a sense control *eno2* cRNA probe did not label sections (Figure 2B lower panel), and a probe for the oligodendrocyte marker *mpz* showed a non-overlapping hybridization pattern with *eno2*. Cells expressing *mpz* were identified as oligodendrocytes by their smaller size compared with neuronal cells expressing *eno2*, and by their location in the optic tracts, medial longitudinal fasciculus and white matter laminae of the tectum (Figure 2C). These controls confirm the specificity of the *eno2* expression pattern demonstrated by this technique, and show that the widespread hybridization pattern of the *eno2* cRNA probe to brain sections is attributable to pan-neuronal expression of *eno2* rather than non-specific probe hybridization. Northern blot analysis of total RNA samples from whole embryo lysates showed that the 3.5 kb *eno2* transcript was first detected at 48 h post-fertilization (hpf), but its expression level increased markedly between 48 and 72 hpf to reach a maximum at 72 hpf; expression continued at a similar level thereafter (Figure 2D). Weak *eno2* expression was first detected by whole mount RNA *in situ* hybridization in the developing nervous system at 24 hpf (Figure 2E). In agreement with the northern blot analysis, the expression level increased thereafter, such that abundant *eno2* mRNA was readily detected at 72 hpf. Expression was restricted to the nervous system and was most prominent within the brain, spinal cord and retina (Figure 2E). Under identical conditions, no signal was seen when embryos were hybridized with an *eno2* sense control probe (Figure 2E).

Zebrafish *eno2* transcription start site and genomic organization

The expression pattern of zebrafish *eno2* reproduced many of the features that we sought to emulate in a transgenic neurodegeneration model. Consequently, we proceeded to characterize the gene and isolate its *cis*-acting regulatory elements.

We employed 5′rapid amplification of cDNA ends (RACE), using the tobacco acid pyrophosphatase (TAP) method (17), in order to locate the *eno2* transcriptional start site and promoter (Figure 3A). Amplification of cDNA derived from TAP-treated (TAP^+), adapter ligated RNA, using a RACE adapter primer and a gene-specific primer, yielded several products of 300–320 bp. Under the same conditions, no products were generated by amplification of cDNA derived from an identical RNA sample which was not subjected to TAP treatment (TAP^-) before adapter ligation. Using two *eno2* gene-specific primers, instead of the RACE primer, amplification products were generated from both TAP^+ and TAP^- samples. These controls show that the RNA samples and reverse transcription were equivalent between the TAP^+ and TAP^- samples; however, adapter ligation and RACE amplification was dependent on cleavage of the mRNA cap structure by TAP. Consequently, the boundary between the RACE adapter and the *eno2* sequence in the

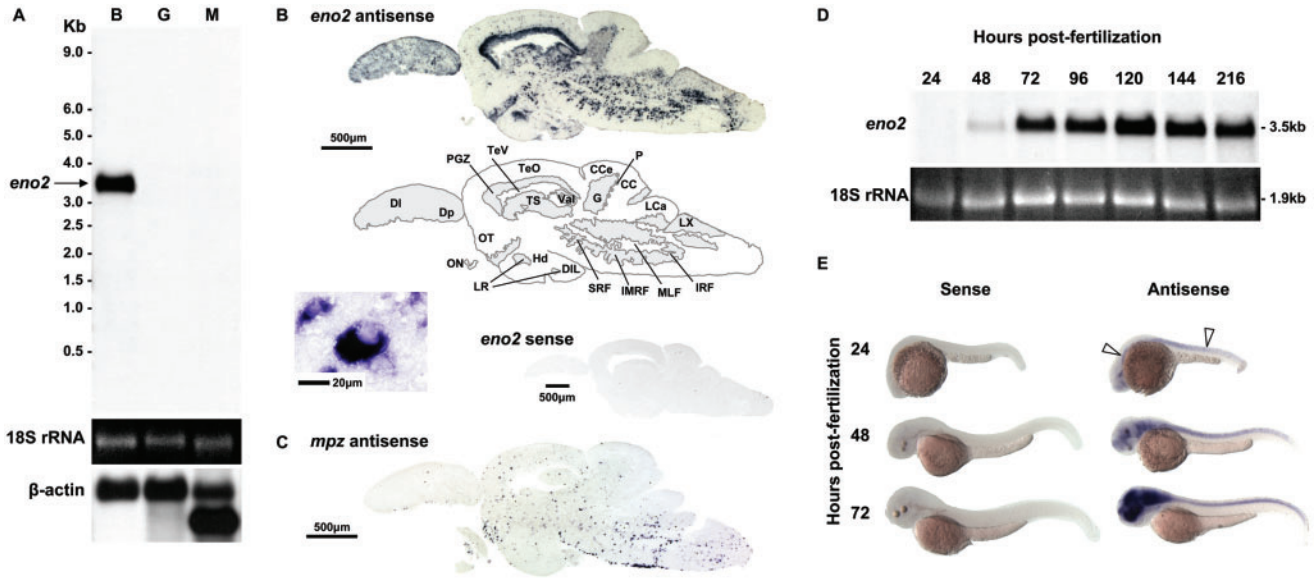

Figure 2. The expression pattern of zebrafish *eno2*. A digoxigenin labelled cRNA probe complementary to the 5′ segment of the *eno2* open reading frame and 5′UTR was used to examine the expression pattern of *eno2* in adult, embryonic and larval zebrafish by northern blot hybridization and RNA *in situ* hybridization. (**A**) Northern blot adult tissues. Total RNA (1.5 μg/lane) derived from adult brain (B), gut and liver (G) and muscle (M) was separated by denaturing gel electrophoresis and the 18S rRNA band photographed (middle panel) to confirm equal sample loading before northern transfer. The blot was probed sequentially with the *eno2* cRNA probe (upper panel) and a probe to β-actin (lower panel). Bound probe was detected using a light-emitting substrate and exposure to photographic film. (**B** and **C**) RNA *in situ* hybridization, adult brain. Parasagittal sections of adult zebrafish brains (rostral left, dorsal up) were hybridized with the *eno2* antisense cRNA probe (B, upper panel and inset), a control sense *eno2* cRNA probe (B, lower panel) or a cRNA probe to an oligodendrocyte marker, *mpz* (C). Hybridized probe was detected using a colorigenic substrate producing a purple reaction product. The morphology of *eno2*-expressing cells was examined at high power (B, inset panel). The topographical locations of cells expressing *eno2* were identified as illustrated in the accompanying schematic (middle panel). Key: Dl, dorsal telencephalon, lateral zone; Dp, dorsal telencephalon, posterior zone; PGZ, periventricular grey zone of optic tectum; TeV, tectal ventricle; TeO, optic tectum; TS, semicircular torus; Val, valvula cerebelli; G, granule cell layer of cerebellum; P, Purkinje cell layer of cerebellum; CCe, corpus cerebellaris; Lca, caudal lobe of cerebellum; LX, vagal lobe; SRF, IMRF, IRF, superior, intermediate and inferior reticular formation; MLF, medial longitudinal fascicle; LR, lateral recess of diencephalic ventricle; Hd, dorsal zone of periventricular hypothalamus; DIL, diffuse nucleus of the inferior lobe; ON, optic nerve (11). (**D**) Northern blot, embryo and larval samples. Total RNA (1.5 μg/lane) from whole embryo/larvae lysates at 24–216 hpf was separated by denaturing gel electrophoresis and the 18S rRNA band photographed (lower panel) to confirm equal sample loading before northern transfer. The blot was probed with the *eno2* antisense cRNA probe under identical conditions to (A). (**E**) Whole mount *in situ* hybridization. AB* zebrafish larvae were fixed and hybridized with the *eno2* antisense cRNA probe (right) or a sense control *eno2* cRNA probe (left). Hybridized probe was detected using the purple colorigenic substrate shown in (B). Lateral views are shown of zebrafish larvae (rostral left, dorsal up) at 24, 48 and 72 hpf. The arrowheads indicate weak hybridizing signal in the developing nervous system of the 24 hpf embryo.

RACE amplification product corresponds to the 5′ boundary of the *eno2* transcript and therefore the transcriptional start site of the *eno2* gene. We cloned the RACE products and sequenced 16 randomly chosen clones. Sequence analysis disclosed the presence of an untranslated first exon in the *eno2* gene, which is located 3.6 kb upstream of exon 2. There are four transcriptional start sites distributed over 28 bp of the promoter sequence (Figure 3B). Examination of the 5′ genomic flanking region did not reveal canonical TATA or CAAT motifs. 3′RACE (Figure 3C) showed a single consensus AUUAAA polyadenylation signal at position 3232 in the transcript, with respect to the most 5′ transcription start site. The full transcript is 3259 nt in length, in agreement with the northern blot data, after allowing for addition of the poly(A) tract. Comparison of the full cDNA sequence with the genomic DNA sequence showed that zebrafish *eno2* is composed of 12 exons distributed over 18.6 kb of genomic sequence (Figure 3D). The boundary between intron 1 and exon 2 is a single nucleotide 5′ of the ATG translational initiation codon, such that the obligatory A residue at position –3 of the Kozak consensus sequence is located within the 3′ end of exon 1 (Figure 3B). The genomic organization of zebrafish *eno2* is very similar to human ENO2, which also contains 12 exons, the first of which is untranslated (35). The length of each protein-encoding exon is identical between human and zebrafish, as are the phases of the splice boundaries with respect to protein translation (Supplementary Data, Table 1). Exon 12 of the zebrafish gene encodes the C-terminus of the protein and a 3′UTR of 1882 bp.

Expression of an *eno2* promoter construct *in vivo*

We identified a genomic BAC clone, zC51M24, from the CHORI21 library, which contained the 5′ end of the zebrafish *eno2* gene and genomic flanking region. We generated reporter constructs in which expression of enhanced green fluorescent protein (GFP) was under transcriptional control of fragments of the 5′ genomic region of zebrafish *eno2*. Constructs in which expression of

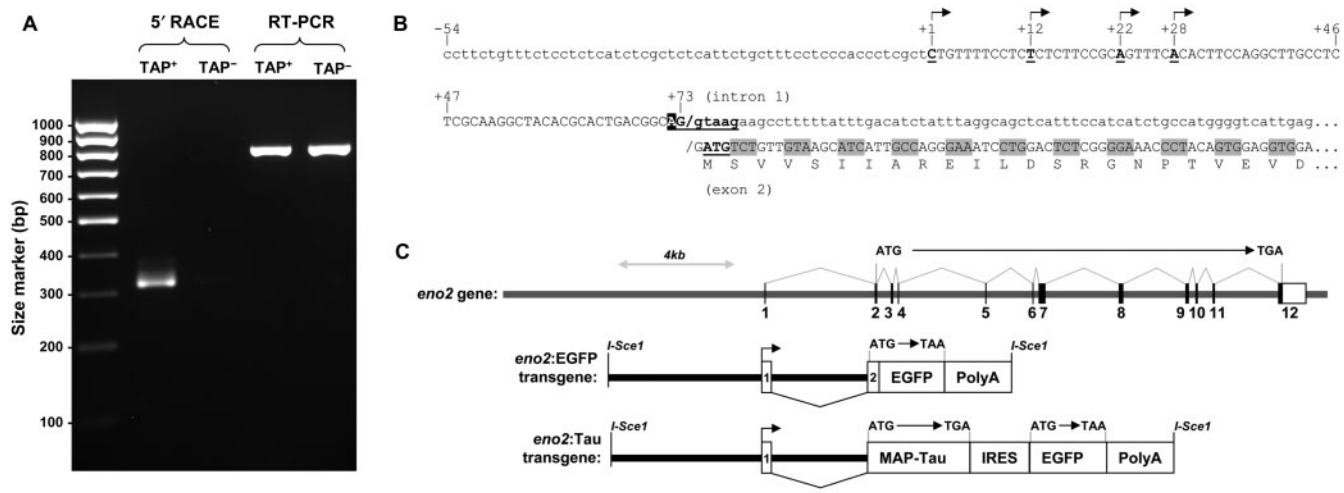

Figure 3. The zebrafish *eno2* gene and promoter. (**A**) 5′RACE was used to map the *eno2* transcription start site. An ethidium bromide stained 1.8% agarose gel is shown. Lane 1: size marker—annotations show size in base pairs. Lanes 2 and 3: first strand cDNA was derived from reverse transcription of RNA that was either treated with TAP (lane 2, TAP^+) or untreated (lane 3, TAP^-), prior to RACE adapter ligation. The cDNA was then amplified by PCR using a RACE adapter 5′ primer and a gene-specific *eno2* 3′ primer. Lanes 4 and 5: TAP^+ (lane 4) and TAP^- (lane 5) first strand cDNA samples, identical to those used as templates for the reactions shown in lanes 2 and 3, were amplified by PCR using two *eno2* gene-specific primers. (**B**) The genomic sequence encompassing the *eno2* promoter. The four transcriptional start sites delineated by 5′RACE are labelled with arrows (+1, +12, +22, +28). Numbering is shown with respect to the most 5′ start site. Exon sequence is shown in upper case; 5′ flanking sequence and intron sequence is shown in lower case. The boundary between exons 1 and 2 at position +73 is shown; the splice donor consensus is underlined. The ATG translational initiation codon in exon 2 is underlined, and the obligate A residue of the Kozak consensus at position −3 with respect to the ATG codon is highlighted in black. (**C**) The schematic illustrates the genomic organization of *eno2* and the DNA constructs used to generate the transgenic zebrafish shown in Figures 4–8.

GFP was under the transcriptional control of up to 4 kb of zebrafish *eno2* genomic sequence 5′ to exon 1 did not show detectable GFP expression in microinjected embryos up to 4 days of age (data not shown). Analysis of the *eno2* genomic sequence using *cpgplot* (http://www.ebi.ac.uk/emboss/cpgplot/), identified a putative CpG island in the first intron of the *eno2* gene, from positions +788 to +988, measured from the 3′ boundary of exon 1 (Supplementary Data, Figure 2). Since CpG islands often overlap important regulatory elements, we incorporated intron 1 into a larger reporter construct (Figure 3C). A 12 kb fragment of the *eno2* gene was captured from the BAC by gap repair recombination, into an acceptor plasmid that contained a GFP-poly(A) cassette fused to the 3′ *eno2* homologous arm. The resulting reporter construct contained 12 kb of the *eno2* gene spanning from 8 kb upstream of exon 1, through intron 1, to exon 2, with eGFP-PolyA inserted in frame into exon 2. The entire cassette was flanked by I-Sce1 meganuclease sites. The plasmid was microinjected into single cell zebrafish embryos, together with I-Sce1 enzyme and buffer (3,36). Starting at around 48 hpf GFP expression was seen in the nervous systems of ~30% of microinjected embryos. A mosaic pattern of expression was evident, allowing microscopic inspection of individual cells. GFP-expressing cells showed neuronal morphology, with individual GFP-expressing cell bodies visible throughout all parts of the central nervous system (Figure 4A). GFP-expressing axons were visible in both the central and peripheral nervous systems. We raised all surviving microinjected fish to sexual maturity; pre-selection for GFP-expressing embryos was not carried out, in order to allow ascertainment of the crude germline transgenesis rate for the technique. We analysed genomic DNA extracted from pooled embryos resulting from outcross of each micro-injected fish with a wild-type control (Figure 4B). A total of 132 adult F0 zebrafish fish were assayed for germline transmission in this manner. Five fish were identified that transmitted the transgene through the germline, suggesting a crude germline transgenesis rate of ~4%. We established transgenic lines from each of these germline mosaic F0 fish. The transgene alleles for each of these lines have been designated Pt401–405 inclusive.

In order to ascertain the relative transgene expression level of each line, we subjected the brains of adult transgenic fish to northern blot analysis. The *eno2* probe shown in Figure 2A hybridized with both the endogenous *eno2* mRNA and the chimeric *eno2-GFP* transcript. The endogenous mRNA acted as a loading control, facilitating comparison of the transgene expression level between different transgenic lines (Figure 4C). Lines Pt401–404 showed a single transgene transcript of expected size, 1.2 kb. Line Pt404 showed the highest expression level in adult brain, Pt402 showed the lowest level; Pt401 and Pt403 showed an intermediate level of expression. Line Pt405 showed an intermediate expression level of the *eno2-GFP* transcript and an additional unexpected 1.6 kb GFP-hybridizing transcript of lower abundance.

The F2 and F3 generations of all five transgenic Tg(*eno2:GFP*) lines showed expression of GFP in the nervous system, in an identical pattern (Figure 4D–F). Weak GFP expression was first detected in the spinal cord and brain at 24–30 hpf and increased thereafter, such that GFP was readily visible by epifluorescence microscopy

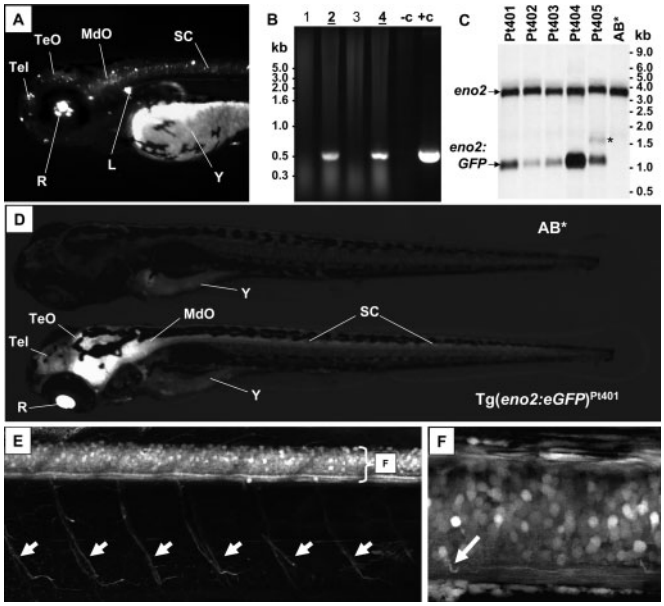

Figure 4. Expression of a 12 kb *eno2* promoter construct in transgenic zebrafish. The 12 kb *eno2:GFP* construct shown in Figure 3C was microinjected into single-cell zebrafish embryos and stable transgenic lines were derived as described in the text. (**A**) Lateral view of the head and rostral trunk region of a microinjected zebrafish larva (rostral left, superior up) at 72 hpf by epifluorescence microscopy, showing punctate mosaic GFP expression. Key: Tel, telencephalon; TeO, optic tectum; MdO, medulla oblongata; SC, spinal cord; R, retina; L, lateral line ganglion. The yolk sac, Y, is autofluorescent. (**B**) Transgenic founders were identified by transmission of the GFP transgene to progeny embryos by genomic PCR. The picture shows an ethidium bromide stained agarose gel. Lanes 2 and 4, genomic DNA from embryos derived from transgenic parents; lanes 1 and 3, genomic DNA from embryos derived from non-transgenic parents; lane 5 ('–c'), genomic DNA from wild-type embryos; lane 6 ('+c'), genomic DNA from wild-type embryos spiked with GFP plasmid. (**C**) Northern blot analysis of GFP expression in stable transgenic lines. Total RNA (1.5 µg/lane) derived from adult brains of each transgenic line was subjected to denaturing gel electrophoresis and northern transfer and the resulting blot hybridized with a probe to *eno2* that is complementary to sequences within both the endogenous *eno2* transcript and the *eno2-GFP* transgene mRNA. The asterisk indicates the unexpected additional hybridizing band detected in line Pt405 and discussed in the text. (**D**) GFP expression in living stable Tg(*eno2:GFP*)^{Pt401} zebrafish larvae by epifluorescence microscopy. An oblique lateral view of an F3 generation Tg(*eno2:GFP*)^{Pt401} larva is shown at 5 days post-fertilization, compared with a wild-type AB* larva (both larvae are orientated rostral left, dorsal up). The yolk sac, Y, is autofluorescent in both larvae. The major GFP-expressing divisions of the nervous system are labelled; the key is the same as (A). (**E**) Lateral confocal microscopic image of the spinal cord and trunk of an F3 generation Tg(*eno2:GFP*)^{Pt404} larva at 5 days post-fertilization. GFP expression is seen within the segmental spinal nerve roots (arrows) and in cell bodies within the spinal cord (bracketed). (**F**) High-power view of spinal cord, showing GFP expression in individual neurons in the spinal grey matter and axons in the ventral funiculus. Occasional GFP-expressing axons (arrow) were seen entering the ventral funiculus from the grey matter.

at 72 hpf. By 5 days post-fertilization, the entire central nervous system was brightly fluorescent (Figure 4C and D), the fluorescent signal filling the outline of the brain and spine. Using confocal microscopy, individual GFP-expressing neurons and their axons were visible in the brain, spine and periphery. GFP-expressing axons were visible within segmental spinal nerve roots, exiting the spinal cord and passing either ventrally and caudally, or dorsally and caudally to innervate somatic muscles and tegument (Figure 4E, arrows). Individual neurons within the grey matter of the developing spinal cord expressed GFP in their cell bodies, and GFP-positive axons were visible running parallel to the long axis of the cord in the ventral funiculus (Figure 4F). Some GFP-expressing neurons within the central spinal grey matter gave rise to axons that entered the ventral funiculus (Figure 4F, arrow). GFP expression was also visible in other neural structures in Tg(*eno2:GFP*) larvae from each line, including the retina, the lateral line nerves and ganglia and peripheral nerves in the facial region (data not shown).

Sections from adult Tg(*eno2:GFP*) brains derived from each of the transgenic lines were examined for GFP expression by indirect IHC (Figure 5A). GFP expression was seen throughout the brain, and was most prominent in the olfactory bulb, telencephalon, optic tectum, Purkinje cell and molecular layers of the cerebellum and the brainstem reticular formation; GFP-expressing cells showed neuronal morphology, with large cell bodies and axons (Figure 5B). We employed double indirect immunofluorescence and confocal microscopy in order to establish the nature of the cells expressing the *eno2*:*GFP* transgene (Figure 5C–F). GFP-expressing cells also expressed a variety of neuronal and neurochemical markers. ChAT-expressing cholinergic neurons in all parts of the brain expressed GFP, the highest levels being evident in large cholinergic neurons of the brainstem. Some groups of inhibitory GABAergic neurons also showed GFP expression (Figure 5F), although many of the clusters of small GABAergic neruons identified in the diencephalon did not show GFP expression. Catecholaminergic neurons were identified by their expression of tyrosine hydroxylase (TH). The most robust GFP expression in catecholaminergic neurons was seen in dopaminergic cells of the olfactory bulbs (Figure 5D); dopaminergic neurons in the pretectal area also exhibited prominent GFP immunoreactivity. Other TH-positive groups showed variable expression of GFP; for example the large dopaminergic neurons of the periventricular hypothalamus did not express detectable GFP (data not shown). Cerebellar Purkinje cells were identified topologically, morphologically and by immunoreactivity for IP3R1; these cells expressed GFP robustly (Figure 5E). In contrast to the widespread expression of *eno2* in different populations of neuronal cells, co-localization of GFP with the glial marker GFAP was not observed (data not shown). A similar pattern of co-localization between GFP and neuronal markers was evident in samples derived from 4-day old transgenic larvae (Supplementary Data, Figure 3). However, at this earlier time point, there was greater variability in GFP expression within groups of morphologically and neurochemically defined groups of neurons.

We examined expression of the GFP transgene outside the CNS, since expression in non-neural tissues might complicate future phenotypic analysis of transgenic lines made using this promoter. By epifluorescence microscopy, non-neural GFP expression in four of five lines (alleles Pt401–404) was limited to the distal extremities of

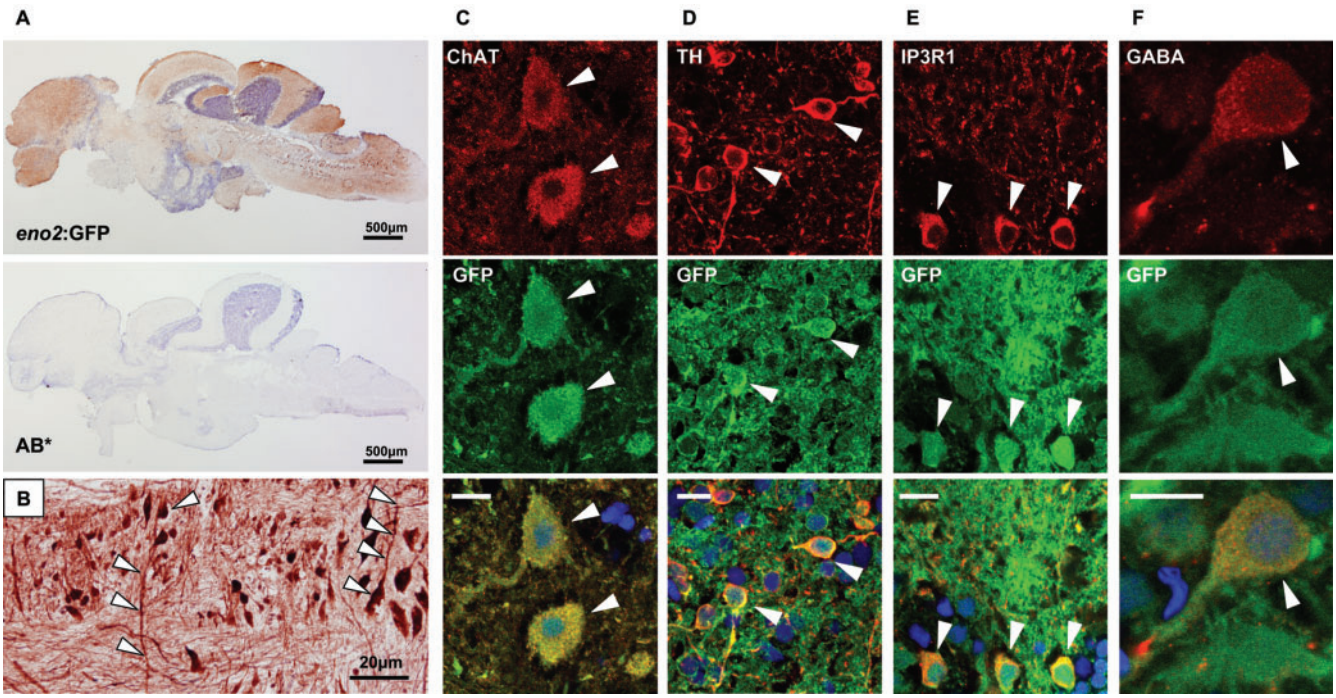

Figure 5. GFP expression in the brains of adult Tg(*eno2:GFP*) zebrafish. (**A**) Parasagittal sections of Tg(*eno2:GFP*)^{Pt404} (upper panel) and wild-type (lower panel) brain were labelled with an antibody to GFP. Bound antibody was detected using a histochemical reaction with a red product and nuclei were labelled with a blue counterstain. GFP expression was apparent throughout the brain of transgenic adults. (**B**) High-power view of medullary reticular formation of Tg(*eno2:GFP*)^{Pt404} zebrafish brain, showing GFP expression in cells with neuronal morphology. The arrows show GFP-expressing neurons with axons in the plane of the section. (**C**–**F**) Double label confocal images of Tg(*eno2:GFP*)^{Pt404} adult brains. Each panel consists of a set of three images: (i) Upper image; red: a cell type-specific marker of interest was localized using specific antibodies. C: Medulla; ChAT, choline acetyltransferase; cholinergic neurons; D: Olfactory bulb; TH, tyrosine hydroxylase; dopaminergic neurons; E: cerebellum; IP3R1, IP3 receptor 1; cerebellar Purkinje cells; D: thalamus; GABA, γ-amino butyric acid; inhibitory neurons; (ii) Middle image, green: GFP expression was localized in the same sections using a GFP antibody; (iii) Lower image: the merged images show co-localization of GFP and the cell type-specific marker (yellow), and were counterstained with DAPI to show nuclei (blue). The scale bar (10 μm) for each set of images is shown in the lower panel.

the developing fins; in three of these lines (Pt401–403), fin expression was faint and transient. In the line with highest CNS expression, Pt404, GFP fluorescence in the fins became fainter with increasing age, but did not disappear. In the remaining line (Pt405), more extensive ectopic expression of GFP was evident in myoseptae, cartilage of the cranium and developing fin rays. We subjected larvae from each transgenic line to RNA *in situ* hybridization using a probe for the GFP mRNA, providing a more sensitive method for demonstrating non-neural expression (Figure 6). Larvae from lines Pt401–403 showed an identical expression pattern; examples from line Pt401 are shown in Figure 6A. Robust expression of GFP mRNA was seen in the nervous system and, between 30 and 48 hpf, in the developing fins. By 72 hpf GFP mRNA was no longer detected in the fins (except along the distal margins of the pectoral fins), corresponding to the transient GFP expression seen by epifluorescence microscopy. Expression outside the nervous system was not otherwise seen in lines Pt401–403. In line Pt404, which showed the highest expression level of GFP in adult brain, GFP mRNA was also abundant in the larval brain and spinal cord. In addition, GFP mRNA was detected in the developing fins at 48 hpf and in the developing gut at 96 hpf (Figure 6B). The weak signal in the gut was only apparent after prolonged development of the histochemical reaction. In line Pt405, widespread expression of GFP mRNA outside the nervous system was seen in a similar distribution to that observed by epifluorescence microscopy, in the fins, myospetae and developing head region. Next, we performed a northern blot analysis of non-neural tissues derived from adult transgenic fish from lines Pt404 and Pt401 (Figure 6D), specifically asking whether the GFP transgene was expressed in the adult gut in line Pt404. Robust GFP expression in the brain was detected by this technique, but GFP mRNA was not detected in gut, muscle or testis from either line, even after 5-fold over-exposure of the blot. The β-actin loading control confirmed that equal amounts of mRNA were loaded in each lane of the blot. The failure to detect GFP mRNA in the gut of adult Tg(*eno2:GFP*)^{Pt404} fish suggests that expression in the gut during development is transient, or that adult gut expression occurs at a very low level, beyond the limit of detection by this technique. Finally, we examined intact adult fish by epifluorescence microscopy (Figure 6E). Lines Pt404 and Pt405 showed persistent weak expression of GFP along the extreme distal margins of the fins. In addition, fluorescent sensory nerve axons in the peripheral nervous

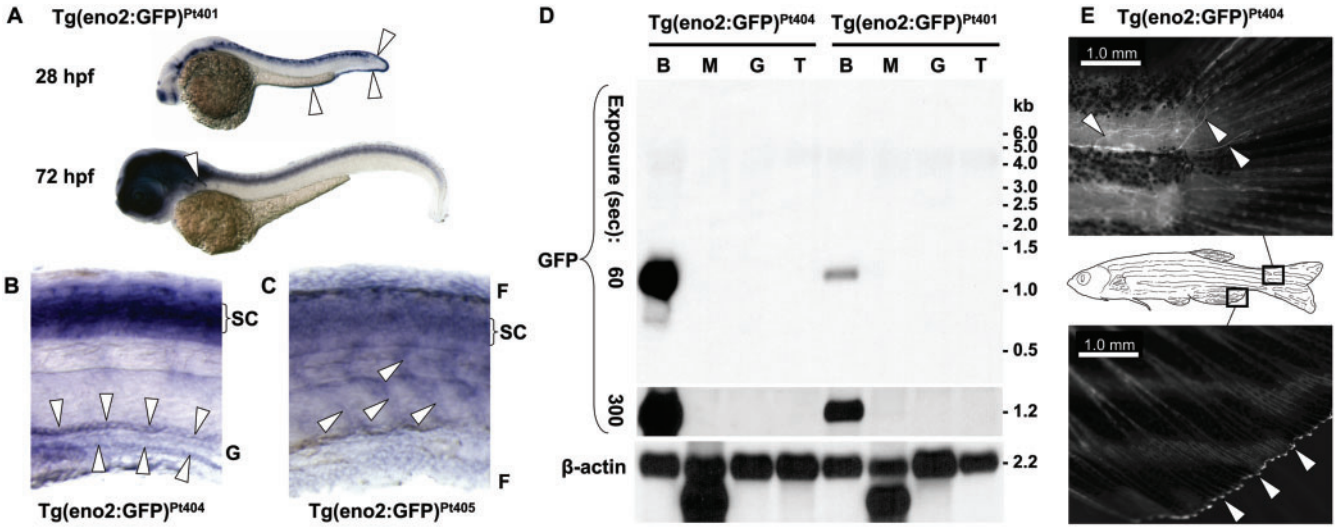

Figure 6. GFP expression outside the central nervous system of Tg(*eno2:GFP*) zebrafish. (**A**) Tg(*eno2:GFP*)^{Pt401} larvae at 28 and 72 hpf were subjected to RNA *in situ* hybridization using a cRNA probe complementary to GFP. The arrowheads indicate GFP mRNA expression in the developing fins in the 28 hpf embryo, and in the distal margins of the pectoral fins in the 96 hpf larva. (**B**) High-power view of the trunk region of a Tg(*eno2:GFP*)^{Pt404} larva at 96 hpf. Key: SC, spinal cord; G, gut. The arrowheads indicate weak expression of the transgene in the developing intestine. (**C**) High-power view of the trunk region of a Tg(*eno2:GFP*)^{Pt405} larva at 96 hpf. Key: SC, spinal cord; F, fins. The arrowheads indicate ectopic expression of the transgene in myoseptae. (**D**) Northern blot analysis of tissues derived from adult Tg(*eno2:GFP*)^{Pt404} and Tg(*eno2:GFP*)^{Pt401} zebrafish. Key: B, brain; M, muscle; G, gut; T, testis. Two micrograms total RNA from each tissue was subjected to denaturing electrophoresis and northern transfer. The blot was probed using a cRNA probe to GFP and exposed for 60 s (upper panel) or 5 min (middle panel). The blot was then re-probed with a cRNA probe to β-actin (lower panel). (**E**) Epifluorescence microscopy of an adult Tg(*eno2:GFP*)^{Pt404} zebrafish. High-power views are shown of the caudal peduncle region (upper panel) and distal anal fin (lower panel). Arrowheads indicate GFP expression in sensory nerves (upper panel) and distal fin margins (lower panel).

system were visible through the dermis of adult Tg(*eno2:GFP*)^{Pt404} zebrafish.

These data show that the 12 kb *eno2* promoter fragment drives transgene expression in neurons throughout the CNS, including neuronal populations of specific interest to neurodegenerative disorders, such as cerebellar Purkinje cells, dopaminergic neurons and cholinergic neurons. Expression starts at 24–30 hpf, but does not reach maximal levels until around 72 hpf, after the major divisions of the nervous system are formed and when functioning neurons expressing markers of differentiation are present. Expression outside the nervous system is limited, occurring transiently in the fins and at very low levels in the gut. This promoter element may, therefore, be useful in constructing transgenic zebrafish models of neurodegenerative disease.

Transgenic fish expressing 4-repeat Tau under the *eno2* promoter

In order to test whether the *eno2* promoter could be used to express genes associated with neurodegeneration, we produced transgenic zebrafish expressing the 4-repeat isoform of human microtubule-associated protein Tau (MAP-Tau4R) (37). MAP-Tau4R contains four carboxy-terminal tandem repeat sequences of 31–32 amino acids within the microtubule binding domain, and is deposited in cerebral neurons in the human neurodegenerative disorders progressive supranuclear palsy and corticobasal degeneration (38). In contrast to the *eno2:GFP* construct described above, which was generated by making a translational fusion between exon 2 of the *eno2* gene and GFP, we were anxious to avoid altering the primary sequence of MAP-Tau4R. Consequently, we used a cDNA encoding MAP-Tau4R to replace the ORF of *eno2* in its entirety, relying on accurate and efficient splicing of the intron present in the chimeric *eno2:MAP-Tau4R* transcript to generate an *eno2:Tau* transcriptional fusion with a Kozak consensus sequence at the translational initiation codon (Figure 3B). In addition, we added an internal ribosome entry site and GFP sequence to the cassette, in order to allow visual genotyping of transgenic fish by fluorescence microscopy. We found that the IRES sequence functions too weakly in fish to be reliably used for this purpose (data not shown), and so we identified zebrafish carrying the transgene by PCR genotyping using the GFP primers shown in Figure 4B. Transgenic Tg(*eno2:Tau*) lines were generated as described above. Heterozygous Tg(*eno2:Tau*) zebrafish larvae comprised a Mendelian fraction of each clutch of eggs and were viable and fertile as adults. The adults are currently 12 months old and show no evidence of increased mortality or reduced fertility in comparison with wild-type zebrafish. A full histological, biochemical and behavioural characterization of Tg(*eno2:Tau*) zebrafish will be reported separately. In the present study, we concentrated on assessing the utility of the zebrafish *eno2* promoter for construction of this type of model, and here we report relevant findings in one line of transgenic zebrafish, designated Tg(*eno2:Tau*)^{Pt406}.

First, we asked whether splicing of *eno2* intron 1 from the chimeric *eno2:Tau* transcript occurred with sufficient efficiency and fidelity to allow expression of the transgene. This is an important consideration, since the transgene sequence was inserted 2 nt downstream of the *eno2* exon 2 splice acceptor, potentially modifying the splicing event. Northern blots were constructed using total RNA from wild-type and Tg(*eno2:Tau*)^{Pt406} zebrafish brains (Figure 7A). An antisense cRNA probe to GFP hybridized with a single 2.5 kb band, which is the expected size of the transgene mRNA after splicing. A duplicate blot was hybridized with a cRNA probe to *eno2* exons 1–3. As expected, this detected the endogenous 3.5 kb *eno2* transcript in both wild-type and transgenic samples, but also hybridized with a 2.5 kb RNA from transgenic brain, suggesting that the 2.5 kb species is formed by splicing of intron 1 from the chimeric transcript. The primary transcript derived from the transgene is predicted to be 6.5 kb in size, and a band of this size was not seen even after prolonged exposure of either blot, indicating that splicing occurred efficiently. It should be noted that the native *eno2* transcript presents 307 nt of sequence complementary to the probe, but the chimeric *eno2-Tau* transcript presents only 72 nt of sequence complementary to the probe. Therefore, the relative abundance of the two transcripts cannot be estimated from the relative signal intensities of the hybridizing bands. In order to examine the fidelity of splicing, we performed RT–PCR, using a 5′ primer complementary to *eno2* exon 1 and a 3′ primer complementary to the human MAP-Tau4R cDNA (Figure 7B). A single 400 bp product, the expected size of the PCR product after intron 1 splicing, was amplified from cDNA derived from Tg(*eno2:Tau*)^{Pt406} zebrafish brain, but not wild-type brain. No other bands were generated, suggesting that splicing occurred accurately at the native boundaries. We cloned the RT–PCR product and sequenced 10 randomly chosen clones (Figure 7C). All 10 clones showed identical sequence spanning the junction between *eno2* exon1 and human 4R-Tau. The junction occurred at an identical location to the exon1–exon2 junction in the native *eno2* mRNA, and accurately re-constituted the Kozak consensus signal for translation of the 4R-Tau transgene. These data confirm that the native *eno2* intron 1 splice signals were operational even after the replacement of exon 2 with a heterologous transgene sequence.

We next asked whether the resulting *eno2-Tau* transcript was translated to produce detectable protein. Western blot analysis was undertaken using lysates from Tg(*eno2:Tau*)^{Pt406} zebrafish brains, wild-type zebrafish brains and human post-mortem cerebral cortex (Figure 8A). Equal amounts of protein were loaded in each lane and the blot was sequentially probed using: (i) a monoclonal antibody that recognizes all splice isoforms of human MAP-Tau, but which does not react with zebrafish microtubule-associated proteins, followed by: (ii) an actin antibody that recognizes both the human and zebrafish proteins. Bands representing the six reported human MAP-Tau isoforms were evident in the human cortex sample (37). A single abundant band corresponding to the MAP-Tau4R transgene was observed in the sample

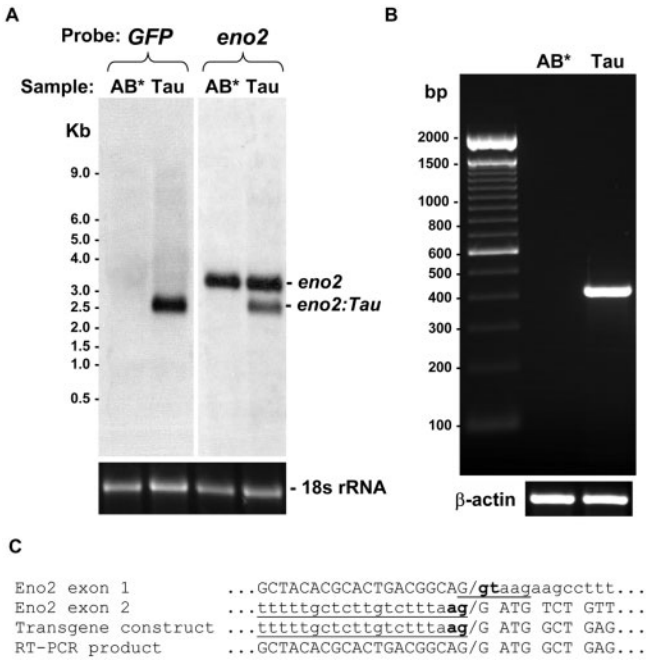

Figure 7. Splicing of intron 1 from a chimeric *eno2:Tau* transcript *in vivo*. Stable transgenic zebrafish were generated using the *eno2:Tau* transgene shown in Figure 3C. (**A**) Two micrograms of total RNA derived from Tg(*eno2:Tau*)^{Pt406} ('Tau') or wild-type ('AB*') adult zebrafish brains was separated by denaturing gel electrophoresis and the 18S rRNA band photographed (lower panel) to confirm equal sample loading before northern transfer. Duplicate blots were probed using digoxigenin-labelled cRNA probes complementary to GFP (left blot) or *eno2* (right blot), as shown in Figure 2A. The endogenous *eno2* and chimeric *eno2:Tau* transcripts are labelled. (**B**) An ethidium stained 1.8% agarose gel is shown; lane 1 contains DNA marker, annotations show size in base pair. Total RNA, derived from Tg(*eno2:Tau*)^{Pt406} (lane 2, 'Tau') or wild-type (lane 3, 'AB*') adult zebrafish brains, was subjected to reverse transcription followed by PCR amplification using a 5′ primer specific for *eno2* exon 1 and a 3′ primer specific for human 4R-Tau (upper panel). Aliquots of the same cDNA samples were then subjected to PCR amplification using two β-actin primers (lower panel). (**C**) The eno2-Tau PCR product from (B) was cloned and sequenced. The schematic shows the exon 1 splice donor and exon 2 splice acceptor sequences from the endogenous *eno2* gene, the chimeric *eno2:Tau* splice acceptor, and the sequence of the eno2-Tau RT-PCR product across the boundary between the *eno2* and human Tau sequences.

derived from Tg(*eno2:Tau*)^{Pt406} zebrafish brain; this was not seen in the sample derived from control zebrafish brain. Densitometric measurement suggested that the transgenic fish brain expressed 8–10-fold higher levels of MAP-Tau relative to the β-actin control than human cortex. These data suggest that the *eno2* promoter drives high-level transgene expression in adult zebrafish brain. To ascertain the expression pattern of transgenic 4R-Tau, we undertook a preliminary histological examination of adult Tg(*eno2:Tau*)^{Pt406} zebrafish brains (Figure 8B). IHC, using the primary antibody used in Figure 8A, showed widespread expression of human MAP-Tau4R throughout Tg(*eno2:Tau*)^{Pt406}, but not wild-type, zebrafish brain. The transgene product was readily detectable owing to its abundant expression. For example, in the optic tectum, large afferent axons parallel to the pial surface of the brain

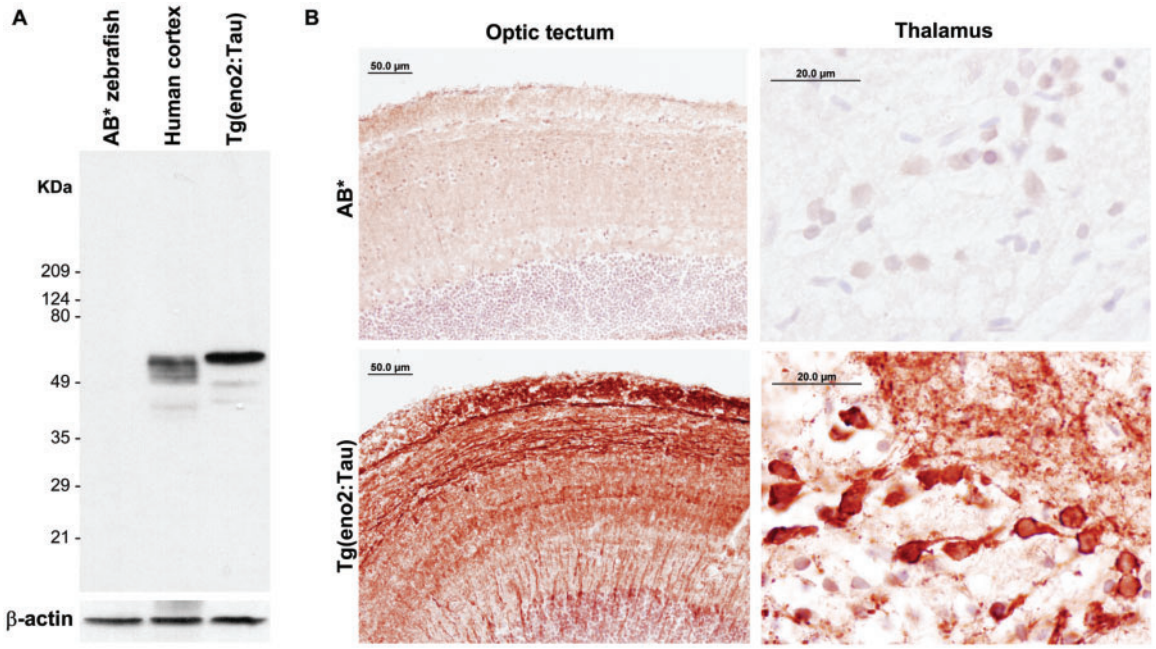

Figure 8. Expression of 4R-Tau in the brains of adult Tg(*eno2:Tau*) zebrafish. (**A**) Ten micrograms of protein derived from wild-type AB* zebrafish brain, normal human post-mortem cerebral cortex or Tg(*eno2:Tau*)^{Pt406} zebrafish brain was separated by SDS–PAGE and transferred to a PVDF membrane. The resulting western blot was probed sequentially with an antibody specific to human Tau (upper panel) and an antibody that binds to both human and zebrafish actin (lower panel). (**B**) Sections from wild-type AB* (upper two panels) or Tg(*eno2:Tau*)^{Pt406} (lower two panels) zebrafish brains were immunolabelled using the human Tau-specific antibody shown in (A). Bound antibody was detected using a peroxidase-conjugated secondary antibody and a histochemical reaction with a red reaction product, as shown in Figure 5A. Nuclei were counterstained blue. The left two panels show low-power views of the optic tectum to demonstrate the regional pattern of Tau expression in axons and neuropil. The right two panels show high-power views of the thalamus to demonstrate expression of Tau in the cell bodies and proximal processes of neurons, which are identified by their large pale-staining nuclei.

in the superficial laminae, and large axons perpendicular to the pial surface in the deep laminae were densely labelled with the Tau antibody (Figure 8B, lower left panel). In addition, the neuropil was heavily labelled, as were neurons in multiple laminae. High-power examination revealed abnormal cytoplasmic expression of Tau in many neurons (Figure 8B, lower right panel). Neuronal somatic Tau immunolabelling was dense and showed a refractile pattern suggestive of fibrillar deposition in several areas, including the thalamus. These findings resembled neurofibrillary tangles and neuropil threads seen in human tauopathies.

These data show that the 12 kb *eno2* promoter element drives expression of a heterologous transgene in neurons of the zebrafish brain at sufficiently high levels to allow detection of the transgene product pathologically and biochemically, and the generation of histological changes reminiscent of human disease.

DISCUSSION

Mammalian and fish enolase genes

Zebrafish *eno2* and mammalian ENO2 share extensive homology, including regulatory sequences, genomic organization and predicted amino acid sequences. The genes are likely derived from a common ancestor, and the demonstration of other zebrafish enolase genes predicting proteins with homology to mammalian α- and β-enolase isoenzymes suggests that the gene duplications that presumably led to distinct functionally specialised enolase isoenzymes occurred before fish and mammals diverged in evolution. The conserved neuronal expression pattern of *eno2* suggests that γ-enolase might have specific functions in neurons. Two putative *eno1* orthologues were found in zebrafish. An ENO1 processed pseudogene is present within the human genome (39), but it shows characteristics of sequence inserted by reverse transcription, in particular lacking introns. This was not the case in the zebrafish genes, and it seems likely that the zebrafish has two copies of the *eno1* gene.

Expression of an ENO2 orthologue in zebrafish has been previously described in a high-throughput *in situ* hybridization analysis (accessible on line: Thisse and Thisse 2004, http://zfin.org/cgi-bin/webdriver?MIval=aa-markerview.apg&OID=ZDB-GENE-040704-27). The expression pattern described in the present study is similar to the previous work, except that an earlier time of onset of expression in trigeminal ganglia, and expression in developing myotomes, was described in the earlier study. A likely explanation for these minor differences relates to the probe sequences used in the studies. We selected a short (307 nt) probe complementary to the 5′ end of the *eno2* transcript because it showed no cross-hybridization with other enolase transcripts, whereas probes complementary to the 3′ end of the *eno2* open reading frame

showed cross hybridization with *eno1* and *eno3*. The probe used in the high-throughput study was generated from a plasmid containing 1379 bp of the *eno2* open reading frame. Although the greater length of this probe likely enhanced its sensitivity for detecting low-level expression at earlier time points, our data suggest that this may have been at the expense of specificity.

The *eno2* regulatory region

Similar to the human and rat genes, the zebrafish *eno2* promoter lacks canonical TATA, CAAT or initiator sequences, shows multiple transcriptional start sites, and the gene contains an untranslated first exon that is spliced to a second exon containing the ATG translational initiation codon (35,40). Approximately 40% human genes have untranslated first exons (41), and there are several examples of genes in which important regulatory elements lie in the first intron following an untranslated first exon (42). In the zebrafish gene, we found a putative 200 bp CpG island in the first intron; analysis of the rat and human first introns similarly showed short CpG islands. Although the introns from the three different species showed very limited sequence conservation overall, the CpG islands were more highly conserved (human-rat 64%, human-zebrafish 46%; Supplementary Data, Figure 2). A previously reported *in vitro* analysis of the rat NSE promoter suggested that there may be a neuron-specific enhancer sequence within the first intron of the rat gene (43). Our data in transgenic fish *in vivo* are compatible with the similar presence of neuronal regulatory elements in the first intron of the zebrafish *eno2* gene, suggesting phylogenetic conservation of an intronic neuronal enhancer. The important elements could be delineated by deletion analysis, to establish whether the phylogenetically conserved sequences are necessary or sufficient for promoter activity and specificity.

Previous attempts to construct transgenic murine models of Alzheimer's disease used a 1.8 kb fragment of the rat NSE promoter to drive expression of the amyloid precursor protein β-APP. The transgene was expressed at insufficient levels to reproduce the full pathological profile of Alzheimer's disease in transgenic animals (44,45). The 1.8 kb rat NSE construct likely contains a small subset of the *cis*-acting signals that contribute to physiological expression levels of the native transcript, and lacks the regulatory elements present in the first intron of the rat gene. This might account for its failure to drive expression at sufficient levels to provoke pathology. The 12 kb zebrafish *eno2* promoter fragment expressed the human MAP-Tau gene in hemizygous transgenic animals at 8-fold higher levels than in human brain. The 12 kb fragment contains the putative neuronal intronic enhancer; in addition a generic intron enhances transgene expression levels in transgenic animals (46,47), possibly through mechanisms other than the presence of transcriptional regulatory regions within the intron, such as linked intron splicing and nuclear mRNA export (48,49).

Despite the 12 kb *eno2* promoter construct expressing transgenes at high levels, it does not contain all of the *cis*-acting signals present in the zebrafish gene, since the reporter transgene does not fully recapitulate the expression pattern of the endogenous transcript. Thus, in adult Tg(*eno2:GFP*) brain from each of the lines, little GFP expression was visible in the cerebellar granule cell layer, even though the endogenous transcript was abundantly expressed in this brain region. Large fragments of the regulatory region of the murine ENO2 gene are required to recapitulate the physiological gene expression pattern in mice; a 250 kb BAC reporter containing the entire murine ENO2 locus, showed expression of the transgene in a similar pattern to the endogenous gene (50). Two further transgenic lines in which transgene expression was driven by a 25 kb genomic fragment only partially recapitulated the expression pattern of the endogenous transcript. Interestingly, one of the principal differences between the 25 kb and 250 kb regulatory elements was loss of transgene expression in the granule cells of the cerebellum with the smaller construct. This is similar to the pattern we observed in Tg(*eno2:GFP*) zebrafish, in which GFP expression was absent from the cerebellar granule cell layer, despite expression of the endogenous gene in this region. This suggests that sequences responsible for γ-enolase expression in cerebellar granule cells lie remote from the immediate 5′ region of the gene in both mouse and zebrafish. We saw ectopic GFP expression in Tg(*eno2:GFP*) embryos in the distal margins of the fins in non-neural structures. This expression was presumably due to the absence of an important non-neural repressor element in the 12 kb *eno2* transgene construct, since we observed the finding in multiple independent transgenic lines. In addition, weak ectopic GFP expression was observed in the gut of Tg(*eno2:GFP*)^{Pt404} larvae. It is unclear whether this is attributable to absence of an important promoter element or to an artefact arising from the site of genomic integration, since we did not observe expression in the gut of other transgenic lines. However, Pt404 shows the highest expression level and so might be the only line in which low-level 'leaky' promoter activity was detectable in the intestine. Ectopic expression in myoseptae and cartilage of Tg(*eno2:GFP*)^{Pt405} larvae was presumably a result of a genomic integration site artefact, since transgene expression was not seen in these locations in other lines. Interestingly, an unexpected *eno2* hybridizing band was seen on northern blot analysis of brain RNA derived from this line, in addition to the expected endogenous gene and transgene bands. This finding suggests an aberrant splicing event between the transgene and a gene in the vicinity of its genomic integration site, perhaps accounting for the ectopic GFP expression observed in this line.

Meganuclease-mediated transgenesis

The 12 kb *eno2* promoter fragment is sufficiently small that insertion of transgene sequences into the plasmid construct is straightforward; the resulting plasmid can be grown at high copy number in *Escherichia coli* and DNA preparations made with ease. In addition, the relatively compact nature of the construct allows for efficient transgenesis using the I-Sce1 technique. Had we

pre-screened for GFP expression, the germline transgenesis rate amongst microinjection survivors would have been much higher than the 4% we observed; assuming the 4% was a subset of the ~30% that expressed GFP, we might have expected to isolate 10–15% germline transgenics from the GFP-expressing embryos.

Tg(*eno2:GFP*) zebrafish

The stable lines of Tg(*eno2:GFP*) zebrafish generated in the course of this work may be useful for applications demanding *in vivo* visualization of neurons and their axons. NSE expression is generally considered a feature of cells with neuronal differentiation (24). GFP-expressing cells in Tg(*eno2:GFP*) embryos and larvae showed morphological features of mature neurons, and were visible throughout the neuraxis. Later stages of CNS development or the effects of neurotoxins or genetic mutations that cause neurodegeneration could be directly observed in these transgenic zebrafish *in vivo* by epifluorescence microscopy. In addition, peripheral nerve GFP expression was visible through the dermis in adult zebrafish. There are few animal models in which peripheral nerve axons can be directly observed, yet there are a multitude of toxic and metabolic diseases to which these axons are particularly susceptible. Potentially, Tg(*eno2:GFP*) zebrafish might provide a means to directly observe disease progression in models of these pathological processes.

Use of the zebrafish *eno2* promoter to construct transgenic disease models

Our aim was to isolate a *cis*-acting promoter construct that drives an appropriate spatial and temporal transgene expression pattern at a sufficient level to allow its use in the generation of transgenic disease models. The data suggest that the *eno2* promoter fulfils many of the requisite properties for this application:

Spatial expression pattern. We observed expression of the transgene in neurons of the brain, spine, retina and peripheral nervous system in five independent transgenic (*eno2:GFP*) lines. GFP expression was evident in neuronal populations of specific relevance to the study of neurodegeneration, for example cerebellar Purkinje cells, motor neurons and dopaminergic neurons. This spatial pattern is appropriate for studying the differential susceptibility of subgroups of neurons to proteins expressed ubiquitously in neurons. One possible concern for the use of the *eno2* promoter in transgenic disease models relates to ectopic expression of the transgene in non-neuronal cells at the distal margins of the fins and also at low levels in the developing gut. The fins are robustly regenerative in the zebrafish; we routinely use tail fin biopsy as a means to obtain genomic DNA to determine the genotype of transgenic zebrafish, and the fins regenerate rapidly afterwards. It is very unlikely that an adverse phenotype relating to the expression of transgene in the distal fin margins will impinge on the successful generation of fish with neurodegenerative disease biochemistry. It is also doubtful that the ectopic expression of transgenes in the intestine, at the low level we observed relative to robust CNS expression, will be deleterious to the future generation of disease models. Other promoters successfully used for generating rodent models of neurodegenerative disease show ectopic expression outside the CNS, for example weak expression of the PrP promoter in the kidney and heart (51). Furthermore, many human neurodegenerative disease genes are expressed ubiquitously, but seem to exert toxic effects selectively in neurons.

Temporal expression pattern. Expression of the 12 kb *eno2* promoter starts at 24–28 hpf, but increases significantly between 48 and 72 hpf and persists through adulthood. The relatively late onset of high-level expression may avoid potentially deleterious effects of early transgene expression on the initial differentiation of neurons, but will encompass the later stages of larval development when screening approaches can still be deployed practicably. Persistence of expression into adulthood will allow examination of age-related progression of pathology in transgenic fish.

Expression levels. We were concerned that transgene expression from the 12 kb *eno2* promoter relies on accurate and efficient splicing of the *eno2* first intron from a chimeric transcript in which the second exon is replaced by a cDNA sequence of interest and the remainder of the *eno2* transcript is missing. However, our studies show that splicing of intron 1 from the chimeric transcript occurs with high efficiency and fidelity, accurately aligning the 3′ end of exon 1 with the ATG signal in exon 2, resulting in a Kozak consensus sequence. This allowed efficient translation of the transgene, with steady-state levels of the Tau transgene being several fold higher than the native protein in human brain tissue. We have now used this promoter to express a variety of transgenes and have observed similar findings in multiple transgenic lines. The presence of the intron in the promoter construct significantly contributes to robust transgene expression.

In summary, we have cloned and characterized a zebrafish *eno2* promoter fragment, demonstrated its utility in driving transgene expression in a neuronal pattern in stable transgenic animals, and used it to generate a zebrafish Tauopathy model. Our current studies are focussed on establishing whether Tg(*eno2:Tau*) zebrafish develop a full spectrum of phenotypic changes reminiscent of human Tauopathies.

SUPPLEMENTARY DATA

Supplementary Data are available at NAR Online.

ACKNOWLEDGEMENTS

We are grateful to the following colleagues for generously sharing reagents: Dr Neal Copeland (NCI, Frederick, MA; DY380 cells); Dr Matthew Farrer (Mayo Clinic, Jacksonville, FL; 4R-Tau plasmid); Dr Michael Tsang (University of Pittsburgh, PA; pBS-I-Sce1) and Dr Steven T. DeKosky (Alzheimer's Disease Research Centre,

P50 AG05133, University of Pittsburgh, PA; normal human brain lysate). We thank Paula Chalmers and Gretchen Blasko (University of Pittsburgh Division of Laboratory Animal Resources) for expert care of our zebrafish stocks.

FUNDING

This work was supported by research grants from: The Society for Progressive Supranuclear Palsy (ref #441-2005); the University of Pittsburgh Competitive Medical Research Fund; the Pittsburgh Institute for Neurodegenerative Diseases; and a research gift from Mr Henry Fisher. Funding to pay the Open Access publication charges for this article was provided by University of Pittsburgh Medical Center, Department of Neurology.

Conflict of interest statement. None declared.

REFERENCES

1. Kimmel,C.B. (1989) Genetics and early development of zebrafish. *Trends Genet*., **5**, 283–288.
2. Peters,K.G., Rao,P.S., Bell,B.S. and Kindman,L.A. (1995) Green fluorescent fusion proteins: powerful tools for monitoring protein expression in live zebrafish embryos. *Dev. Biol*., **171**, 252–257.
3. Thermes,V., Grabher,C., Ristoratore,F., Bourrat,F., Choulika,A., Wittbrodt,J. and Joly,J.S. (2002) I-SceI meganuclease mediates highly efficient transgenesis in fish. *Mech. Dev*., **118**, 91–98.
4. Amsterdam,A., Burgess,S., Golling,G., Chen,W., Sun,Z., Townsend,K., Farrington,S., Haldi,M. and Hopkins,N. (1999) A large-scale insertional mutagenesis screen in zebrafish. *Genes Dev*., **13**, 2713–2724.
5. Guo,S., Wilson,S.W., Cooke,S., Chitnis,A.B., Driever,W. and Rosenthal,A. (1999) Mutations in the zebrafish unmask shared regulatory pathways controlling the development of catecholaminergic neurons. *Dev. Biol*., **208**, 473–487.
6. Burns,C.G., Milan,D.J., Grande,E.J., Rottbauer,W., MacRae,C.A. and Fishman,M.C. (2005) High-throughput assay for small molecules that modulate zebrafish embryonic heart rate. *Nat. Chem. Biol*., **1**, 263–264.
7. Goldsmith,P. (2004) Zebrafish as a pharmacological tool: the how, why and when. *Curr. Opin. Pharmacol*., **4**, 504–512.
8. Peterson,R.T., Shaw,S.Y., Peterson,T.A., Milan,D.J., Zhong,T.P., Schreiber,S.L., MacRae,C.A. and Fishman,M.C. (2004) Chemical suppression of a genetic mutation in a zebrafish model of aortic coarctation. *Nat. Biotechnol*., **22**, 595–599.
9. Stern,H.M., Murphey,R.D., Shepard,J.L., Amatruda,J.F., Straub,C.T., Pfaff,K.L., Weber,G., Tallarico,J.A., King,R.W. *et al.* (2005) Small molecules that delay S phase suppress a zebrafish bmyb mutant. *Nat. Chem. Biol*., **1**, 366–370.
10. Zon,L.I. and Peterson,R.T. (2005) In vivo drug discovery in the zebrafish. *Nat. Rev. Drug Discov*., **4**, 35–44.
11. Wullimann,M.F., Rupp,B. and Reichert,H. (1996) *Neuroanatomy of the Zebrafish Brain*. Birkhauser Berlin.
12. Ma,P.M. (2003) Catecholaminergic systems in the zebrafish. IV. Organization and projection pattern of dopaminergic neurons in the diencephalon. *J. Comp. Neurol*., **460**, 13–37.
13. Koulen,P., Janowitz,T., Johnston,L.D. and Ehrlich,B.E. (2000) Conservation of localization patterns of IP(3) receptor type 1 in cerebellar Purkinje cells across vertebrate species. *J. Neurosci. Res*., **61**, 493–499.
14. Westerfield,M., McMurray,J.V. and Eisen,J.S. (1986) Identified motoneurons and their innervation of axial muscles in the zebrafish. *J. Neurosci*., **6**, 2267–2277.
15. Brosamle,C. and Halpern,M.E. (2002) Characterization of myelination in the developing zebrafish. *Glia*, **39**, 47–57.
16. Kawai,H., Arata,N. and Nakayasu,H. (2001) Three-dimensional distribution of astrocytes in zebrafish spinal cord. *Glia*, **36**, 406–413.
17. Bai,Q., Mullett,S.J., Garver,J.A., Hinkle,D.A. and Burton,E.A. (2006) Zebrafish DJ-1 is evolutionarily conserved and expressed in dopaminergic neurons. *Brain Res*., **1113**, 33–44.
18. Karlovich,C.A., John,R.M., Ramirez,L., Stainier,D.Y. and Myers,R.M. (1998) Characterization of the Huntington's disease (HD) gene homologue in the zebrafish Danio rerio. *Gene*, **217**, 117–125.
19. Son,O.L., Kim,H.T., Ji,M.H., Yoo,K.W., Rhee,M. and Kim,C.H. (2003) Cloning and expression analysis of a Parkinson's disease gene, uch-L1, and its promoter in zebrafish. *Biochem. Biophys. Res. Commun*., **312**, 601–607.
20. Anichtchik,O.V., Kaslin,J., Peitsaro,N., Scheinin,M. and Panula,P. (2004) Neurochemical and behavioural changes in zebrafish Danio rerio after systemic administration of 6-hydroxydopamine and 1-methyl-4-phenyl-1,2,3,6-tetrahydropyridine. *J. Neurochem*., **88**, 443–453.
21. Bretaud,S., Lee,S. and Guo,S. (2004) Sensitivity of zebrafish to environmental toxins implicated in Parkinson's disease. *Neurotoxicol. Teratol*., **26**, 857–864.
22. Lam,C.S., Korzh,V. and Strahle,U. (2005) Zebrafish embryos are susceptible to the dopaminergic neurotoxin MPTP. *Eur. J. Neurosci*., **21**, 1758–1762.
23. McKinley,E.T., Baranowski,T.C., Blavo,D.O., Cato,C., Doan,T.N. and Rubinstein,A.L. (2005) Neuroprotection of MPTP-induced toxicity in zebrafish dopaminergic neurons. *Brain Res. Mol. Brain Res*., **141**, 128–137.
24. Marangos,P.J. and Schmechel,D.E. (1987) Neuron specific enolase, a clinically useful marker for neurons and neuroendocrine cells. *Annu. Rev. Neurosci*., **10**, 269–295.
25. Forss-Petter,S., Danielson,P.E., Catsicas,S., Battenberg,E., Price,J., Nerenberg,M. and Sutcliffe,J.G. (1990) Transgenic mice expressing beta-galactosidase in mature neurons under neuron-specific enolase promoter control. *Neuron*, **5**, 187–197.
26. Mucke,L., Masliah,E., Johnson,W.B., Ruppe,M.D., Alford,M., Rockenstein,E.M., Forss-Petter,S., Pietropaolo,M., Mallory,M. *et al.* (1994) Synaptotrophic effects of human amyloid beta protein precursors in the cortex of transgenic mice. *Brain Res*., **666**, 151–167.
27. Masliah,E., Westland,C.E., Rockenstein,E.M., Abraham,C.R., Mallory,M., Veinberg,I., Sheldon,E. and Mucke,L. (1997) Amyloid precursor proteins protect neurons of transgenic mice against acute and chronic excitotoxic injuries in vivo. *Neuroscience*, **78**, 135–146.
28. Li,Y., Carlson,E., Murakami,K., Copin,J.C., Luche,R., Chen,S.F., Epstein,C.J. and Chan,P.H. (1999) Targeted expression of human CuZn superoxide dismutase gene in mouse central nervous system. *J. Neurosci. Methods*, **89**, 49–55.
29. Kercher,L., Favara,C., Chan,C.C., Race,R. and Chesebro,B. (2004) Differences in scrapie-induced pathology of the retina and brain in transgenic mice that express hamster prion protein in neurons, astrocytes, or multiple cell types. *Am. J. Pathol*., **165**, 2055–2067.
30. Brecht,W.J., Harris,F.M., Chang,S., Tesseur,I., Yu,G.Q., Xu,Q., Dee Fish,J., Wyss-Coray,T., Buttini,M. *et al.* (2004) Neuron-specific apolipoprotein e4 proteolysis is associated with increased tau phosphorylation in brains of transgenic mice. *J. Neurosci*., **24**, 2527–2534.
31. Offen,D., Kaye,J.F., Bernard,O., Merims,D., Coire,C.I., Panet,H., Melamed,E. and Ben-Nun,A. (2000) Mice overexpressing Bcl-2 in their neurons are resistant to myelin oligodendrocyte glycoprotein (MOG)-induced experimental autoimmune encephalomyelitis (EAE). *J. Mol. Neurosci*., **15**, 167–176.
32. Higashijima,S., Okamoto,H., Ueno,N., Hotta,Y. and Eguchi,G. (1997) High-frequency generation of transgenic zebrafish which reliably express GFP in whole muscles or the whole body by using promoters of zebrafish origin. *Dev. Biol*., **192**, 289–299.
33. Braissant,O. and Wahli,W. (1998) A simplified in situ hybridisation protocol using non-radioactively labeled probes to detect abundant and rare mRNAs on tissue sections. *Biochemica*, **1**, 10–16.
34. Saitou,N. and Nei,M. (1987) The neighbor-joining method: a new method for reconstructing phylogenetic trees. *Mol. Biol. Evol*., **4**, 406–425.
35. Oliva,D., Cali,L., Feo,S. and Giallongo,A. (1991) Complete structure of the human gene encoding neuron-specific enolase. *Genomics*, **10**, 157–165.

36. Grabher,C., Joly,J.S. and Wittbrodt,J. (2004) Highly efficient zebrafish transgenesis mediated by the meganuclease I-SceI. *Methods Cell Biol.*, **77**, 381–401.
37. Goedert,M., Spillantini,M.G., Jakes,R., Rutherford,D. and Crowther,R.A. (1989) Multiple isoforms of human microtubule-associated protein tau: sequences and localization in neurofibrillary tangles of Alzheimer's disease. *Neuron*, **3**, 519–526.
38. Arai,T., Ikeda,K., Akiyama,H., Shikamoto,Y., Tsuchiya,K., Yagishita,S., Beach,T., Rogers,J., Schwab,C. *et al.* (2001) Distinct isoforms of tau aggregated in neurons and glial cells in brains of patients with Pick's disease, corticobasal degeneration and progressive supranuclear palsy. *Acta Neuropathol. (Berl)*, **101**, 167–173.
39. Ribaudo,M.R., Di Leonardo,A., Rubino,P., Giallongo,A. and Feo,S. (1996) Assignment of enolase processed pseudogene (ENO1P) to human chromosome 1 bands 1q41–>q42. *Cytogenet. Cell Genet.*, **74**, 201–202.
40. Sakimura,K., Kushiya,E., Takahashi,Y. and Suzuki,Y. (1987) The structure and expression of neuron-specific enolase gene. *Gene*, **60**, 103–113.
41. Davuluri,R.V., Grosse,I. and Zhang,M.Q. (2001) Computational identification of promoters and first exons in the human genome. *Nat. Genet.*, **29**, 412–417.
42. Burton,E.A., Tinsley,J.M., Holzfeind,P.J., Rodrigues,N.R. and Davies,K.E. (1999) A second promoter provides an alternative target for therapeutic up-regulation of utrophin in Duchenne muscular dystrophy. *Proc. Natl Acad. Sci. USA*, **96**, 14025–14030.
43. Sakimura,K., Kushiya,E., Ogura,A., Kudo,Y., Katagiri,T. and Takahashi,Y. (1995) Upstream and intron regulatory regions for expression of the rat neuron-specific enolase gene. *Brain Res. Mol. Brain Res.*, **28**, 19–28.
44. Quon,D., Wang,Y., Catalano,R., Scardina,J.M., Murakami,K. and Cordell,B. (1991) Formation of beta-amyloid protein deposits in brains of transgenic mice. *Nature*, **352**, 239–241.
45. Malherbe,P., Richards,J.G., Martin,J.R., Bluethmann,H., Maggio,J. and Huber,G. (1996) Lack of beta-amyloidosis in transgenic mice expressing low levels of familial Alzheimer's disease missense mutations. *Neurobiol. Aging*, **17**, 205–214.
46. Palmiter,R.D., Sandgren,E.P., Avarbock,M.R., Allen,D.D. and Brinster,R.L. (1991) Heterologous introns can enhance expression of transgenes in mice. *Proc. Natl Acad. Sci. USA*, **88**, 478–482.
47. Choi,T., Huang,M., Gorman,C. and Jaenisch,R. (1991) A generic intron increases gene expression in transgenic mice. *Mol. Cell. Biol.*, **11**, 3070–3074.
48. Luo,M.J. and Reed,R. (1999) Splicing is required for rapid and efficient mRNA export in metazoans. *Proc. Natl Acad. Sci. USA*, **96**, 14937–14942.
49. Reed,R. and Hurt,E. (2002) A conserved mRNA export machinery coupled to pre-mRNA splicing. *Cell*, **108**, 523–531.
50. Lee,E.C., Yu,D., Martinez de Velasco,J., Tessarollo,L., Swing,D.A., Court,D.L., Jenkins,N.A. and Copeland,N.G. (2001) A highly efficient Escherichia coli-based chromosome engineering system adapted for recombinogenic targeting and subcloning of BAC DNA. *Genomics*, **73**, 56–65.
51. Maskri,L., Zhu,X., Fritzen,S., Kuhn,K., Ullmer,C., Engels,P., Andriske,M., Stichel,C.C. and Lubbert,H. (2004) Influence of different promoters on the expression pattern of mutated human alpha-synuclein in transgenic mice. *Neurodegener. Dis.*, **1**, 255–265.